© IWA Publishing 2020
932

Water Practice & Technology Vol 15 No 4
doi: 10.2166/wpt.2020.075

Monitoring the characteristics and removal of natural organic matter fractions in selected South African water treatment plants

Welldone Moyo[a,*], Nhamo Chaukura[a,b], Machawe M. Motsa[a], Titus A. M. Msagati[a], Bhekie B. Mamba[a], Sebastiaan G. J. Heijman[c] and Thabo T. I. Nkambule[a]

[a] Nanotechnology and Water Sustainability (NanoWS) Research Unit, University of South Africa, Johannesburg, South Africa

[b] Department of Physical and Earth Sciences, Sol Plaatje University, Kimberley, South Africa

[c] Department of Civil Engineering and GeoSciences, Technical University of Delft, Delft, The Netherlands

*Corresponding author. E-mail: welldonemoyo@gmail.com

Abstract

This study used spectroscopic methods to investigate the fate and dynamics of natural organic matter (NOM) as it traverses the treatment train at three water treatment plants (WTPs) in South Africa. The character, quantity, and removability of NOM at specific treatment stages was investigated by measuring changes in dissolved organic carbon (*DOC*) concentration, specific ultra-violet absorbance, *UV* absorbance, various spectroscopic indices, and maximum fluorescence intensity levels. A novel method of identifying and quantifying fluorescent fractions by combining synchronous fluorescence spectroscopy (*SFS*) and Gaussian peak fitting is presented. The dynamics of NOM removal were modeled using *2D-SFS* correlation spectroscopy. Humic and fulvic substances dominated coastal plants and were the most amenable for removal by coagulation as shown by Hermanus WTP (plant H), which had a 42% *DOC* removal at the coagulation stage. Tyrosine-like, tryptophan-like and microbial humic-like substances were degraded or transformed concurrently at plant Flag Bushiole (FB) whereas, at plant H, fulvic-like matter was transformed first followed by tyrosine-like then humic-like matter. Through *2D-SFS*, this study revealed that NOM transformation was varied as a consequence of NOM character, the type and dosage of treatment chemicals used, and WTPs operational parameters.

Key words: 2D correlation spectroscopy, drinking water treatment, natural organic matter, PARAFAC, synchronous fluorescence spectroscopy

Highlights

- A novel method of identifying and quantifying fluorescent fractions by combining synchronous fluorescence spectroscopy and Gaussian peak fitting is presented.
- The character of NOM at source and plant operational parameters play a role in the treatability of NOM.
- Synergies of optical methods in tracking changes of NOM fractions due to water treatment processes.

Water Practice & Technology Vol 15 No 4
doi: 10.2166/wpt.2020.075

Graphical Abstract

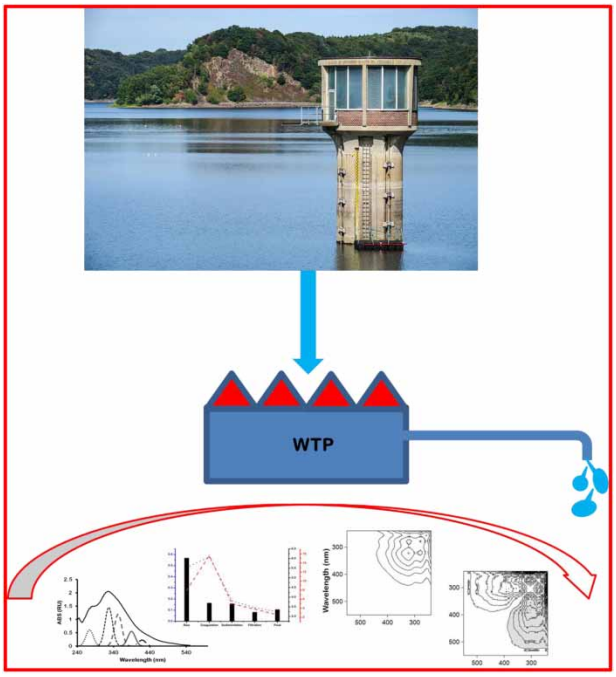

INTRODUCTION

Natural organic matter (NOM) is a complex mixture of organic compounds derived from decaying matter of terrestrial and or aquatic origin found in all natural waters. The source, climatic conditions and land use influence NOM concentrations and reactivity among different natural waters (Moyo *et al.* 2019). NOM is a precursor of disinfection byproducts (DBPs) such as haloacetic acids (HAAs) and trihalomethanes (THMs), which are carcinogenic. Moreover, NOM removal processes and disposal can be expensive, hence there is need for effective real-time monitoring and control techniques. This implies robust and sensitive analytical methods that can provide rapid information on NOM dynamics, reactivity and treatability need to be developed (Ncibi & Matilainen 2018).

Optical methods such as fluorescence excitation emission matrix (*FEEM*) spectroscopy with parallel factor (*PARAFAC*) analysis and ultraviolet-visible (*UV-Vis*) spectroscopy are widely used to characterize the origin, composition and reactivity of NOM. In particular, *UV-Vis* spectroscopy has been applied in tracing and tracking the origin, composition and reactivity of chromophoric dissolved organic matter (*CDOM*) in natural water (Zha *et al.* 2014). NOM-metal interactions and the generation of DBPs after chlorination have been tracked by the log-transformed absorbance (*LnA*) spectra, a variation of processed *UV-Vis* spectra (Li & Hur 2017). *FEEM* with *PARAFAC* analysis has been employed to fingerprint fluorescent dissolved organic matter (*FDOM*) fractions and sources of *DOM* (Ndiweni *et al.* 2019). *PARAFAC* analysis has proved advantageous over other chemometric techniques in analyzing fluorescence data because it can pick up and resolve minute variations in *EEM* datasets by extracting overlapping autonomous fluorophore groups (Hur & Cho 2012). However, complex mixtures such as NOM restrict the application of conventional fluorescence methods because of extensive spectral overlaps that reduce their sensitivity (Murphy *et al.* 2011).

To overcome spectral overlap and interference, techniques such as synchronous fluorescence spectroscopy (*SFS*) can be used. In *SFS*, individual fluorophores are decoupled from a pool of fluorescent NOM fractions in a sample by selecting an appropriate offset wavelength ($\Delta\lambda$) between excitation and emission wavelengths (Yu *et al.* 2013). This technique has been successfully used to study the seasonal

Water Practice & Technology Vol 15 No 4
doi: 10.2166/wpt.2020.075

variation of NOM in a Moorland water (Goslan 2003), and the influence of coagulation and ozonation on the character of effluent organic matter (Jeong *et al.* 2014). Further selectivity of *SFS* can be enhanced by combining it with two-dimensional correlation (*2D-SFS*) to resolve overlapping peaks. This is achieved by extrapolating the peaks over to the second dimension, and discriminating the chronological order of any subtle spectral changes brought about by external perturbations (Su *et al.* 2016).

Most studies have focused on the use of *UV-Vis* spectroscopy and fluorescent spectroscopy or *SFS* in detecting changes of NOM without investigating clear synergies among these methods (Gonçalves-araujo *et al.* 2016; Li & Hur 2017). Herein, we propose the assessment of NOM using complementary optical methods for tracking the transformation of NOM throughout the treatment trains of selected water treatment plants (WTPs) in South Africa. This study aimed at conducting a comparative assessment of the dynamics of NOM removal using combined optical techniques on samples collected after treatment stages. The objectives were: (1) to investigate the occurrence, distribution and fate of NOM fractions and subsequent transformations brought about by treatment processes; and (2) to determine the synergies of optical methods in tracking changes of NOM fractions due to water treatment processes.

MATERIALS AND METHODS

Sampling

Water sampling was performed at three water treatment plants, namely: Flag Busheilo (FB) located inland, Hermanus (H) located on the south east coast, and Mthwalume (MT) located on the eastern coast (Figure A1). More information on the plants is found in the supplementary section (Tables A1 and A2). Triplicate samples were abstracted after each water treatment step using clean 1 L glass bottles with Teflon-lined screw caps. Potable multimeters were used onsite to measure conductivity, temperature, turbidity and pH. Ice boxes were used to transport the samples; upon arrival, a 0.45 μm GF/F filters were used to filter the samples thereafter stored at 4 °C and analysis was conducted within 48 h of sampling. The dissolved organic carbon (*DOC*) of all samples was determined using a total organic carbon analyser (TOC fusion, Teledyne Tekmar).

UV absorbance and fluorescence EEMs

Before analysis, samples were equilibrated to 25 °C then filtered through 0.45 μm GF/F filters. *UV-Vis* absorbance spectra, simulated synchronous scans at a wavelength offset of $\Delta\lambda = 60$ nm, and fluorescence *EEMs* were acquired using a fluorescence spectrometer (Aqualog, HORIBA, Jobin Yvon) in the wavelength range 200–800 nm. The excitation interval was set at 2 nm and the emission was recorded between 248.58–830.59 nm with an emission interval of 3.28 nm. The Raman water peak area was used to calibrate and correct the measured intensities and convert to Raman units (RU) from arbitrary units (AU). This was achieved by exciting the Raman water standard at an excitation wavelength of 350 nm and measuring the emission readings between 248.58 to 830 nm (Ndiweni *et al.* 2019).

Spectroscopic indices such as humification index *(HIX)*, fluorescence index *(FI)* and freshness index *(β:α)* were calculated according to the methods by Lidén *et al.* (2017). *SUVA* ($L.mg^{-1}.m^{-1}$) was derived as a quotient of *DOC* ($mg{\cdot}L^{-1}$) and UV_{254} (m^{-1}) absorbance (Equation (1)).

$$SUVA = \frac{UV_{254}}{DOC} \times 100 \quad (1)$$

Water Practice & Technology Vol 15 No 4
doi: 10.2166/wpt.2020.075

Modeling techniques employed to track NOM composition and dynamics

Log-transformed absorbance spectra

At each treatment stage, the log-transformed absorbance *(LnA)* was obtained by determining the natural logarithm of the measured absorbance. The differential log-transformed absorbance *(DLnA)* spectra were obtained by calculating the difference of the *LnA* of two consecutive treatment stages (Li & Hur 2017) (Equation (2)):

$$DLnA(\lambda_i) = LnA_{i-1} - LnA_i(\lambda) \tag{2}$$

where $A_i(\lambda)$ and $A_{i-1}(\lambda)$ were the measured absorbance intensities of samples collected from two consecutive treatment process at a particular wavelength, respectively.

PARAFAC modeling

The inbuilt SOLO software (Eigenvector Inc.) in the Aqualog instrument was used to perform *PARAFAC* analysis using the method described by Ndiweni *et al.* (2019). In brevity, *PARAFAC* is a modeling technique that relies on statistics to decompose a dataset of *EEMs* into a residual array and a set of trilinear terms (Ndiweni *et al.* 2019) (Equation (3)):

$$x_{ijk} = \sum_{f=1}^{F} a_{if} b_{jk} c_{kf} + e_{ijk} \tag{3}$$

where, i = 1……..I; j = 1……..J and k = 1……..K

The variable x_{ijk} represents the *i*th sample fluorescence intensity set at excitation and emission of *k* and *j* wavelength, respectively. The parameter a_{if} varies with the quantity of the *f*th fluorophore contained in the *i*th sample (the score), and the emission and excitation spectrum of the *f*th fluorophore are denoted by the variables b_{jk} and c_{kf}, respectively (the loadings) (Ndiweni *et al.* 2019). The variable e_{ijk} denotes the residual variables of the model while the variable *F* denotes the number of components making up the fluorophore. Alternating least squares regression procedure was used to fit the model. The maximum fluorescence intensities (F_{max}) were used to quantify the fluorophores after each treatment stage.

Gaussian fitting

Deconvolution and Gaussian peak fitting of the *SFS* spectra was performed using PeakFit v4.12 curve-fitting software. The location of the maxima, intensity, and energy of each Gaussian peak identified the contributing NOM fraction fluorophore and characterized the extent and efficiency of each treatment process. Prior research revealed that these bands have a Gaussian nature when converted to photon energy (Equation (4)) (Li & Hur 2017):

$$E(eV) = \frac{1240}{\lambda(nm)} \tag{4}$$

Two dimensional correlation spectroscopy

Two-dimensional correlation synchronous fluorescence spectroscopy was conducted to determine the rate of compositional variation of NOM due to the impact of treatment using the 2DShige software

Water Practice & Technology Vol 15 No 4
doi: 10.2166/wpt.2020.075

available from Kwansei-Gakuin University website, Japan. The order of treatment was the external perturbation. Briefly, Noda's rules state that only auto peaks are positive whereas cross peaks can either be positive or negative. A positive cross peak in the synchronous spectra with the wavelength pair λ_1/λ_2 means changes occurring at λ_1 and λ_2 are concurrent or synchronous, while a negative cross peak in the synchronous spectra with the wavelength pair of λ_1/λ_2 means changes occurring at λ_1 and λ_2 are inverse or asynchronous. Cross peaks can only be found in the asynchronous spectra. A positive cross peak of λ_1/λ_2 wavelength pair means the pace of change occurring at wavelength λ_1 is faster than that at λ_2 in the asynchronous spectra. A negative cross peak of λ_1/λ_2 wavelength pair within the asynchronous spectra implies that changes occurring at λ_1 are slower than that at λ_2.

Statistical analyses

Correlation and regression analyses were carried out using the XLSTAT software. Analysis of correlations between variables were evaluated using established methods in literature as reported by Najafzadeh & Zeinolabedini (2018, 2019) and Zeinolabedini & Najafzadeh (2019).

RESULTS AND DISCUSSION

Characteristics of NOM components at source using synchronous scan and peak fitting

Gaussian fitting on SFS was processed to identify underlying bands making up the spectra (Figure 1). A near fit of the measured data and the Gaussian distribution bands was observed ($R^2 > 0.95$). All *2D-SFS* scans showed a prominent peak and three characteristic shoulders for all sampled water sources. Peak A was located within the wavelength range 260–314 nm, and ascribed to protein-like matter (PLM) (Hur *et al.* 2011). Peak B was responsible for the second shoulder in the wavelength range of 314–355 nm. This peak is mainly associated with microbial humic-like matter (MHLM) (Yu *et al.* 2013). The fulvic-like matter (FLM) component (Peak C) was the prominent peak for coastal plants (H and MT) and situated in the wave range 355–420 nm (Yu 2011). The humic-like matter (HLM) (Peak D and E) was in the wavelength range 420–500 nm, and was the third and not so prominent shoulder (Yu *et al.* 2013). Overall, the *SFS* scan identified a single peak and three shoulders, defined as PLM, MHLM, FLM, and HLM. The area under the *SFS* graph in a specific wavelength region has been used by most researches to enumerate the relative quantities of the fluorescent components in that specific wavelength region (e.g., Hur *et al.* 2011; Yu *et al.* 2013). This work reports on quantifying fluorescent components as proportional to the area of the resolved Gaussian curve in the respective fluorescence regions.

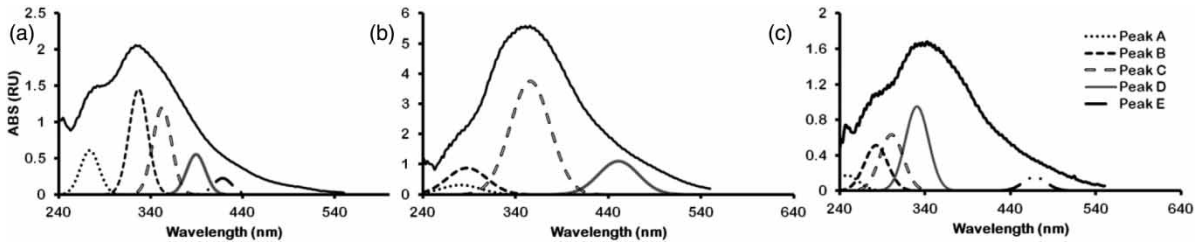

Figure 1 | Synchronous fluorescence spectra with peak fitting for NOM raw water samples for (a) FB, (b) H and (c) MT.

It was interesting to observe that peaks A and B for plant H (16.83 and 47.71 RU, respectively) doubled that of MT (6.40 and 19.05 RU, respectively), despite MT having higher *DOC* levels

Water Practice & Technology Vol 15 No 4
doi: 10.2166/wpt.2020.075

(12.52 mg/L C) and both these plants being located at the coasts. This finding proves the complexity of NOM. This could mean raw water from MT was less microbially impacted at the source than H ($FI = 1.52$ and $FI = 1.38$, respectively) (Table A2), suggesting the supply of *DOC* in MT was perhaps made up of biopolymers, which are non-fluorescent and not easily taken up by microorganisms (Kimura *et al.* 2018). Strikingly, peak C (FLM) was prominent in plant H (200.94 RU), about ten times more intense than MT and FB (23.01 and 30.59 RU, respectively). These results confirm the hypothesis that the brownish-yellowish colouration of feed water to plant H is characteristic of water laden with fulvic acids, as reported by Nkambule (2012). Of interest, peaks for HLM (Peaks D and E) was almost double those for coastal plants H and MT (59.98 RU and 43.93 RU, respectively) compared to inland plant FB (29.81 RU). This further confirms previous results that coastal plants contain feed water laden with humics (Nkambule 2012). Previous research done in South Africa indicated that water from plant H supports microbial growth and proliferation as shown by high BDOC (5 mg/L C), whereas for the other plants the mean value was 2 mg/L C (Nkambule 2012). This suggests microbial growth is supported by HLM because it acts as a substrate for their growth and proliferation, *vis*, high BDOC for plant H (Li *et al.* 2011).

Occurrence and enumeration of fluorescent dissolved organic matter fractions at source

The SOLO software, which is inbuilt into the Aqualog instrument, was used to process fluorescent data for *PARAFAC* using data from all the drinking water sources. This was performed so as to generate a large data pool and to come up with a universal model to cater for any variance among water sources. The aim was to determine the occurrence and quantity of fluorescent NOM fractions at source and to determine how such findings influence downstream processes with regards to NOM treatability. Figure 2 shows the loadings of the obtained spectra of the components. The identity of

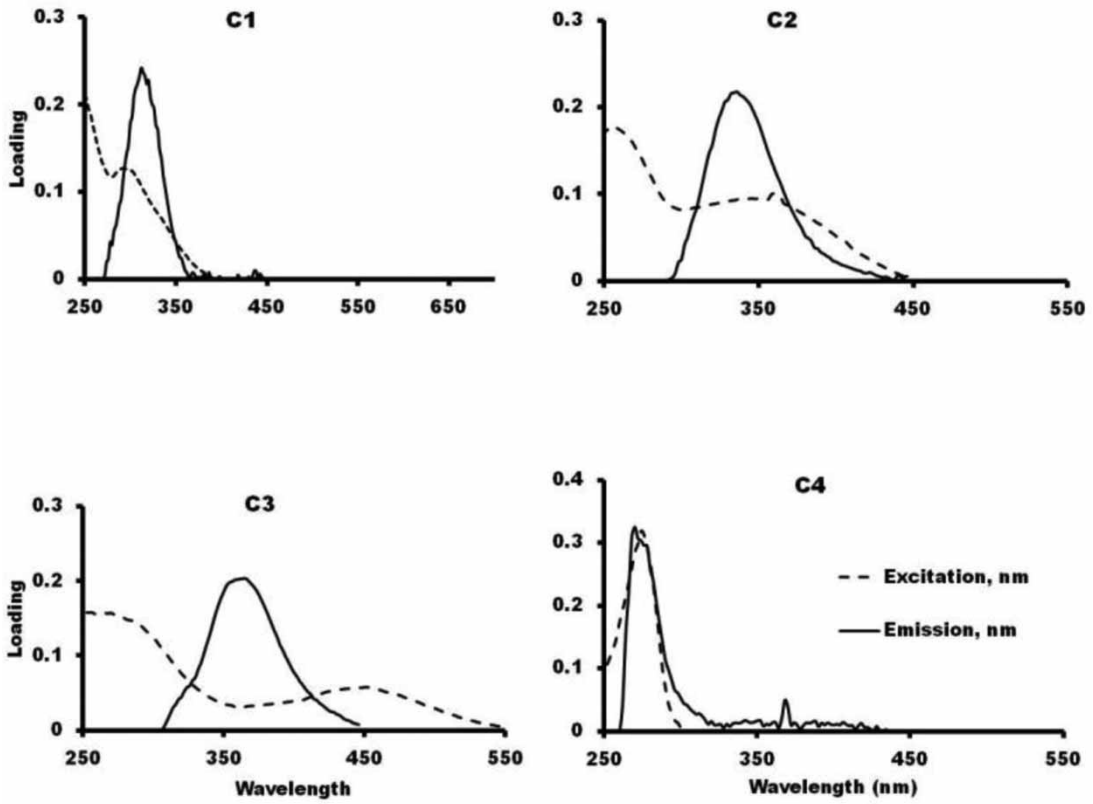

Figure 2 | Loadings for the four PARAFAC components of drinking water samples collected at source.

Water Practice & Technology Vol 15 No 4
doi: 10.2166/wpt.2020.075

contributing fluorophores was ascertained by cross referencing using the OpenFluor database against those obtained globally (Murphy *et al.* 2014).

A split half criteria was used to validate and establish a four component model (Murphy *et al.* 2014). According to the OpenFluor database, components consisted of terrestrial HLM, FLM, and PLM and were denoted as C_1, C_2, C_3 and C_4, respectively. The F_{max} values were used as a measure of the quantity and distribution of the contributing fluorophores. For all water sources, F_{max} was higher for C_1 and C_2 than for C_3 and for C_4 (Table A2). This could mean C_1 and C_2 have high quantum turnover efficiency and low reactions to quenching effects than C_3 and C_4 (Baghoth Sharma & Amy 2010). Of note, F_{max} values for C_2 and C_3 were higher for plant H. The feed water for plant H had a brownish-yellow colouration, mainly signaling the presence of FLM. This is in agreement with the *SFS* results in the previous section. The occurrence and distribution of F_{max} of the tryptophan-like matter (C_4) with origins from autochthonous microbial matter is important because previous research indicated that it is largely predominant in wastewater-impacted waters. The tracking of surface water impacted by wastewater is easily distinguished by the spectral signatures of tryptophan-like matter (Pifer & Fairey 2014). The presence of C_4 therefore signals deliberate or opportune wastewater contamination.

Removal of bulk and specific NOM fractions at different stages of treatment

Dissolved organic carbon

Geographical location of the plants had a bearing on the levels of *DOC* available at source (Figure A1 and Figure 3). This implies catchment activities and bio-geochemical processes influence the quantity and quality of *DOC* found in each of the geographical regions (Ndiweni *et al.* 2019). The *DOC* concentration in the final water for all plants was below the limits laid out by the South African National Standards for water quality (SANS 241), which is $\leq$10 mg/L. The change of NOM quantity and quality as it traverses the treatment train is not adequately traced by *DOC* analysis alone. However, a

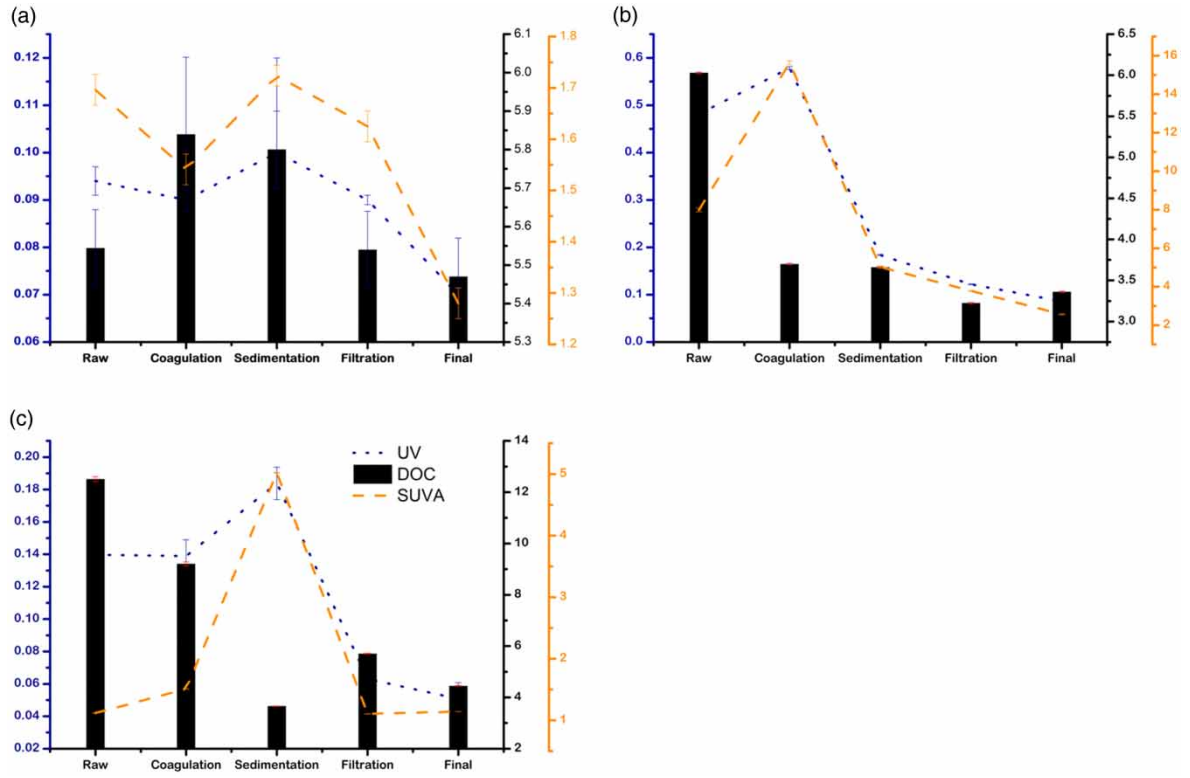

Figure 3 | Chemical properties of water at each treatment stage for (a) FB, (b) H and (c) MT.

Water Practice & Technology Vol 15 No 4
doi: 10.2166/wpt.2020.075

reduction in *DOC* at each treatment stage is a good measure of process efficiency in removing NOM. Coagulation, usually coupled with flocculation, are the major processes attributed to the reduction of *DOC* in conventional WTPs. Similar treatment processes did not guarantee similar *DOC* removal efficiencies among the plants (Table A1 in Supplementary Material). This difference could be a function of coagulant type and dosage, and the character of NOM, or a combination of these (Table A1). Plant H uses alum as a coagulant, and had the highest *DOC* removal efficiency (38.6%). Previous research has shown that the *DOC* in waters laden with HLM, such as plant H, is easily removed by coagulation (Vasyukova *et al.* 2013).

There was an uncharacteristic incline in *DOC* content (5%) at the coagulation stage for FB. This could be the contribution of organic matter from the polymer coagulant used at that plant, which perhaps at the time and point of sampling was not fully mixed. Again there was an uncharacteristic spike in *DOC* concentration (58%) at the filtration stage for plant MT. This was attributed to clogged sand filters due for backwashing. Previous reports indicate that *SUVA* values below 2 $L.mg^{-1}.m^{-1}$ mean the type of NOM is non-humic, and *SUVA* values greater than 4 imply the greater component of NOM in the sample is humic in character. Research has shown that a 50% *DOC* removal is expected when the *SUVA* value is higher than 4 $L.mg^{-1}.m^{-1}$, and a 25% removal is expected when the *SUVA* value is below 2 $L.mg^{-1}.m^{-1}$ (Nkambule 2012). Hence, at the coagulation stage, more than 50% *DOC* removal was expected at plant H, and <25% from plants FB and MT. For plant H, this was close enough (42%), but for plants FB and MT the *DOC* removal at coagulation was - 5 and 31% removal, respectively. It must be noted that these removal guidelines apply at optimal conditions and are dependent on the type and dosage of the coagulants, hence the discrepancy from the guidelines by plants FB and MT (Ncibi & Matilainen 2018).

The analysis of NOM is not routine in South African WTPs because its removal in not prioritized. This work contributes to a new body of knowledge on NOM in the South African context, which can be classified together with DBPs as emerging pollutants of concern. Although the *DOC* concentrations in the treated water were below SANS 241, the critical *DOC* concentration necessary to offset the formation of DBPs is currently not known, therefore routine monitoring is recommended.

UV-Vis

In general, all plants showed a progressive decline in the absorbance at 254 nm from the raw water through to finished final water (Figure 3). From these results it can be inferred that the aromatic composition of the water gradually decreased after every stage for all plants. However, there were anomalies at certain stages of the treatment train where an increase in *UV* absorbance was observed. For example, at the sedimentation stage for plants FB and MT (11 and 29%, respectively). Perhaps this was due to the accretion of suspended and dissolved *UV* absorbing microbial byproducts. The sedimentation basin can act as a batch bioreactor allowing the accumulation of bacteria (Cortina & Gonz 2016). The growth and proliferation of bacteria depends on the aerobic conditions, residence time, temperature and agitation in the basin (Cortina & Gonz 2016). Additionally, irregular cleaning of the sedimentation basin allows for the accumulation of bacteria.

Plant H had the highest UV_{254} absorbance (0.51 cm^{-1}). This means, compared to other plants, the raw water source for plant H was laden with aromatic compounds. From these results, the order of NOM removal measured as UV removal was in the order H (80%) > MT (69%) > FB (32%).

Specific ultraviolet absorbance

Specific ultraviolet absorbance can give a measure of the transphilic, hydrophilic, and hydrophobic character of the NOM in the sample (Nkambule 2012). A *SUVA* value exceeding 4 $L.mg^{-1}.m^{-1}$ implies water is hydrophobic, a *SUVA* value in the range 2 to 4 $L.mg^{-1}.m^{-1}$ implies water is transphilic, and a

Water Practice & Technology Vol 15 No 4
doi: 10.2166/wpt.2020.075

SUVA value below 2 $L.mg^{-1}.m^{-1}$ indicates water of hydrophilic character. Raw water *SUVA* value for plant H was 7.1 $L.mg^{-1}.m^{-1}$, implying hydrophobic moieties dominate the NOM in this sample. The *SUVA* value of the final treated water from that plant was 2.1 $L.mg^{-1}.m^{-1}$ (Figure 3). These results are in agreement with a previous report that indicates NOM in final treated water in South Africa is transphilic in character (Nkambule 2012). There was no significant difference ($p < 0.05$) between the raw and finished waters in terms of *SUVA* change for FB and MT (0.45 and 0.2 unit change, respectively). However, there were significant variations in *SUVA* along the treatment train for these plants. For example, at the sedimentation stage, there was a 3.5 unit increase of *SUVA* for MT. This change from hydrophilic character to hydrophobic character could be due to the accumulation of microbial byproducts as discussed in the preceding section. Notably, the *SUVA* value at coagulation increased by 8 units at the coagulation for plant H, implying the hydrophobic character of NOM increased at this stage. This was unexpected because the hydrophobic NOM fraction has been found to be susceptible to removal by the coagulation process. Such an anomaly could be due to the type of coagulant, in this case alum. The agglomeration and aggregation of NOM as it forms flocs increases its molecular weight and the hydrophobic character (Hoffman *et al.* 2014).

Selective elimination of chromophoric dissolved organic matter fractions

Apart from a monotonic decrease in absorbance, *UV-Vis* spectra for drinking water are usually featureless. Chemometric methods such as differential spectra (*DS*) can be used to process *UV-Vis* data to show more insights on the activity of *CDOM* fractions (Yang *et al.* 2017). Therefore, *DS* can trace and track latent features that could reveal the dynamics of *CDOM* properties after critical stages of water treatment. It is noteworthy that *DS* of a particular treatment process followed the same trend for all plants, therefore respective treatment stages will be discussed together.

All plants showed a decreasing trend from low to high wavelengths at the coagulation stage. At wavelengths less than 290 nm, *UV-Vis* absorbance removal by coagulation was relatively constant, but at wavelengths greater than 290 nm all plants showed a rapid increase (Figure 4). This indicates that coagulation was effective in removing *UV-Vis* absorbing NOM. In addition, this could be because of the transformation occuring from *DOC* to particulate organic matter (POM) as NOM agglomerates into flocs (Yang *et al.* 2017). A correlation of 0.67 was established when considering the efficiency of coagulation as a unit process to remove total CDOM (*tCDOM*) with respect to UV_{254} removal. Such findings were expected because both parameters detect the fraction of NOM that fluoresces. Unexepected, however, was a strong correlation ($R = 0.962$) between total CDOM removal and DOC removal at the coagulation stage. This could be because *DOC* measurement is non selective to both fluorescent and non-fluorescent organic matter. Therefore for these plants, total CDOM removal can be used as a surrogate for *DOC* determination. Similar observations were reported by Wünsch *et al.* 2015. However, seasonal variations should be assessed to test the valididty of this finding.

In the sedimentation and filtration processes, the intensity of the absorbance showed an increasing trend. At these stages, water is retained for a long enough residence time for microorganisms to acclimatise with the environment and produce enzymes necessary to assimilate the available *DOC* in the water (Krzeminski *et al.* 2019). Therefore the increase in *UV-Vis* absorbance could potentially be due to the preference of microorganisms to assimilate low molecular weight NOM fractions from the water, yielding high molecular weight biomolecules as metabolic byproducts.

Typical for chlorinated water, a steady decline in absorbance over the scanned wavelength range after chlorination was observed. *DS* revealed a peak in absorbance in the wavelength region 260–270 nm at this stage (Figure 4). Lavonen *et al.* (2015) reported similar findings and deduced that the absorbance in this range is particularly reactive during disinfection with chlorine or chloroamine. Conjugated double bonds and activated aromatic rings of NOM are disrupted by chlorine at the

Water Practice & Technology Vol 15 No 4
doi: 10.2166/wpt.2020.075

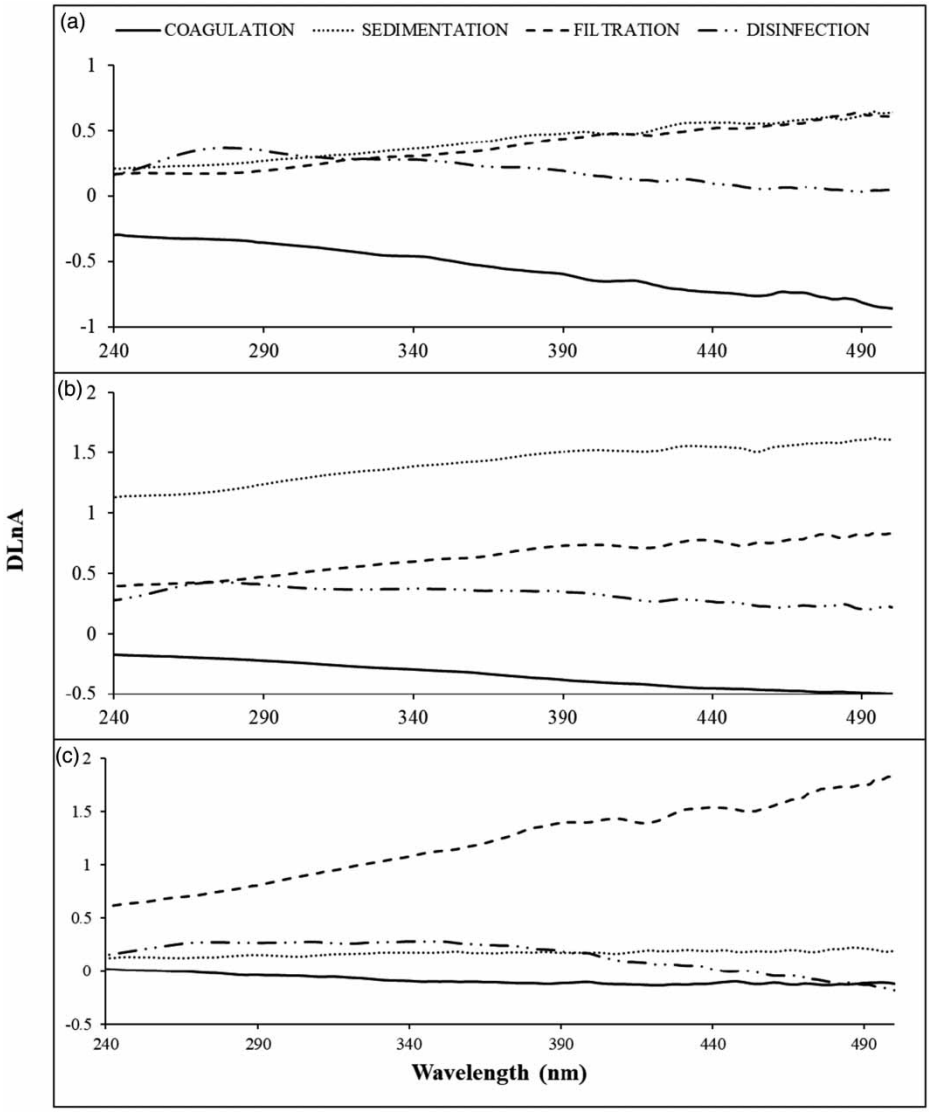

Figure 4 | *DLnA* scans after coagulation, sedimentation, filtration and disinfection for (a) FB, (b) H and (c) MT.

disinfection stage, resulting in the production of smaller and hydrophilic organic substances (Krasner *et al.* 2013).

Tracking compositional variations of DOM due to treatment processes using 2D correlation spectra

Three auto-peaks with the wavelength pairs of 265/265; 295/295 and 335/335 nm were observed in the synchronous 2D correlation spectra for plant FB (Figure 5(a)). The results suggest changes that occurred at wavelengths 265, 295 and 335 nm were concurrent. The peaks at excitation wavelengths of 335, 295 and 265 nm are ascribed to microbial humic-like, tryptophan-like and tyrosine-like matter (Su *et al.* 2016). This implies these NOM fractions were transformed or degraded concurrently down the treatment train. The asynchronous spectra for FB showed positive cross peaks at 380/310, 380/265 and 280/310 nm wavelength pairs (Figure 5(b)), implying the order of change was in the order: 380 → 280 → 265 → 310 nm. The peaks centered at 380 and 310 nm are ascribed to microbial humic-like and tryptophan-like matter while peaks at 280 and 265 are ascribed to tyrosine-like matter (Su *et al.* 2016). For plant H, the synchronous spectra detected a single auto peak at 365/365 wavelength pair (Figure 5(c)), while the asynchronous spectra detected two positive cross

Water Practice & Technology Vol 15 No 4
doi: 10.2166/wpt.2020.075

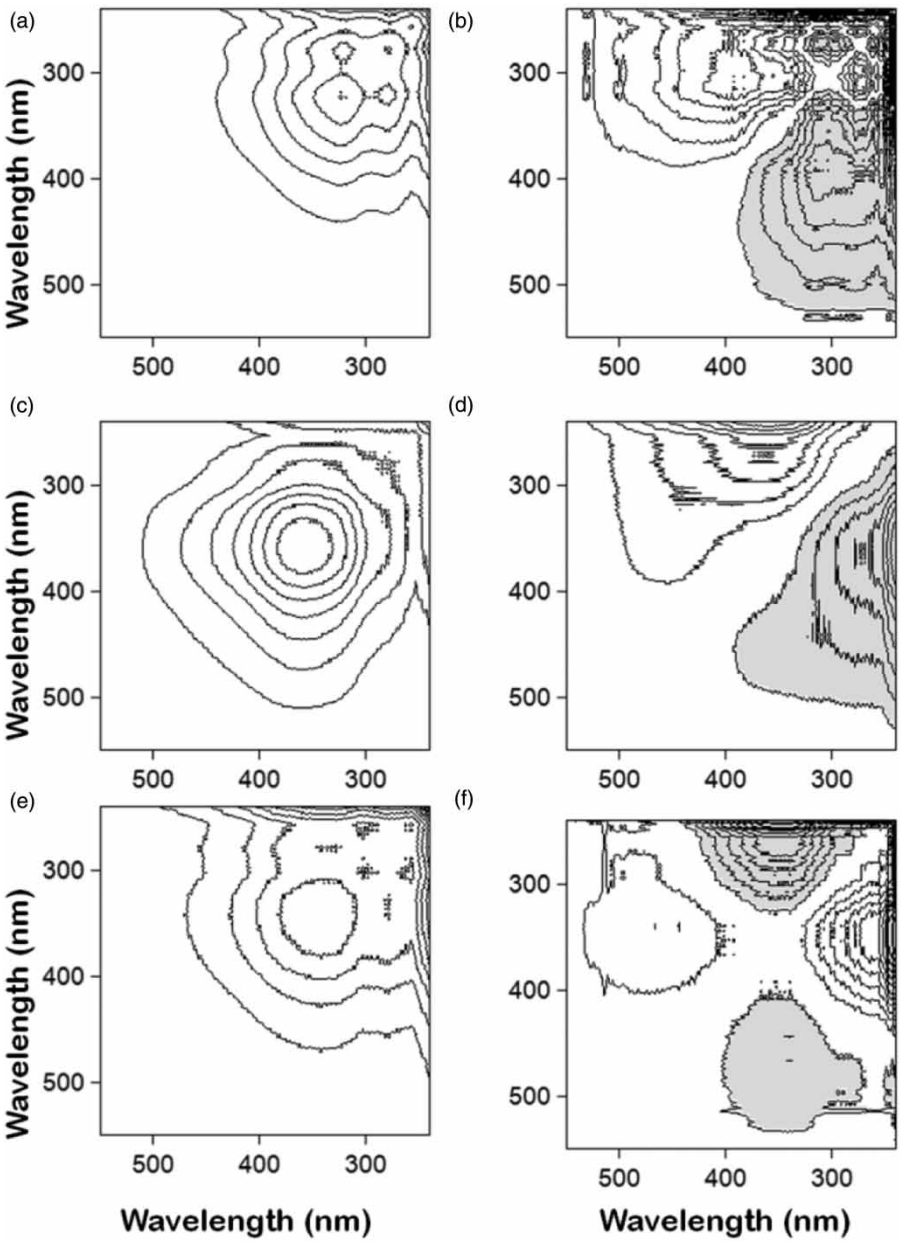

Figure 5 | 2D-SFS of NOM in three water treatment plants: (a) Synchronous 2D correlation map for FB; (b) asynchronous 2D correlation map for FB; (c) synchronous 2D correlation map for H; (d) asynchronous 2D correlation map for H; (e) synchronous 2D correlation map for MT; and (f) asynchronous 2D correlation map for MT. White indicates a positive correlation, and grey indicates negative correlation; a darker shade indicates a stronger correlation.

peaks at the wavelength pairs of 365/265 and 450/365 (Figure 5(d)). According to Noda's rule (Su *et al.* 2016) this means that change at 365 nm is faster than that occurring at 265 nm but slower than that occurring at 450 nm. The peak at 365 nm was ascribed to fulvic-like matter, while peaks at 265 and 450 nm are mainly ascribed to tyrosine-like and humic-like matter, respectively. Therefore the transformation throughout the treatment plant was of the order: 450 → 365 → 265 nm. In the case of plant MT, three auto peaks of wavelength pairs 265/265, 300/300 and 365/365 nm, while two cross peaks of wavelength pairs of 300/265 and 365/280 nm were observed (Figure 5(e)). These results suggest that tyrosine-, tryptophan- and fulvic-like matter were transformed or degraded concurrently throughout the treatment process. Our previous study found tyrosine to be more susceptible to treatment than the other fractions (Moyo *et al.* 2020). This suggests NOM characteristics, treatment regimen and chemicals used play a role in the ease of removal of NOM fractions.

Water Practice & Technology Vol 15 No 4
doi: 10.2166/wpt.2020.075

The asynchronous spectra detected three positive cross peaks at 480/355, 480/295 and 480/265 nm (Figure 5(f)). According to Noda's rule, spectral changes occurring at wavelength 480 are faster than those at 355, 295 and 265 nm. The peak at 480 nm is mainly ascribed to humic-like substances, while those at 355, 295 and 265 nm are ascribed to fulvic-like, tryptophan-like and tyrosine-like matter, respectively (Jarvis 2004).

Correlations relating NOM removal and spectroscopic parameters

A visual Spearman correlation matrix was generated using the XLSTAT statistical software (Figure 6). A correlation matrix gives a visual perspective of correlation data whilst at the same time returning the essential elements of statistical inference. Briefly, patterns are generated which identify both the sign and the intensity if correlations exist: positive correlations are identified by lines that slant from bottom left to top right whilst a negative correlation is depicted by lines which slant from bottom right to top left. The closer to each other the lines are, the closer the correlation is to zero. A mild correlation between the humification index *(HIX)* and UV_{254} removal was established ($R = 0.796$) (Figure A.2a). The *HIX* is associated condensed fluorescence organic matter, hence lower H:C ratios therefore serve as a perfect surrogate for humicity, suggesting its changes to be correlated to UV_{254} absorbance coefficient (Kamjunke *et al.* 2016). *HIX* for the raw water serves as an indicator of its susceptibility to removal by downstream processes. Raw water with a high *HIX* value corresponds with high quantities of humic substances. Humic substances are known to be easily removed by coagulation. Thus it is expected that higher *HIX* must translate to a larger NOM removal. Again the freshness index *(β:α)* correlated fairly with UV_{254} removal ($R = 0.786$) (Figure A.2b). The freshness index (ß:α), therefore changes in the ß:α ratio are expected to correlate with UV_{254} absorbance coefficient (Kamjunke *et al.* 2016). Conventional methods such as coagulation can easily remove NOM with low β:α values. A low β:α index indicates condensed and aged humic matter. The fluorescence index (*FI*) gives the ratio of terrestrially derived organic matter, usually lower values (e.g., degraded soil and plant organic matter) and microbially derived organic matter, usually higher values

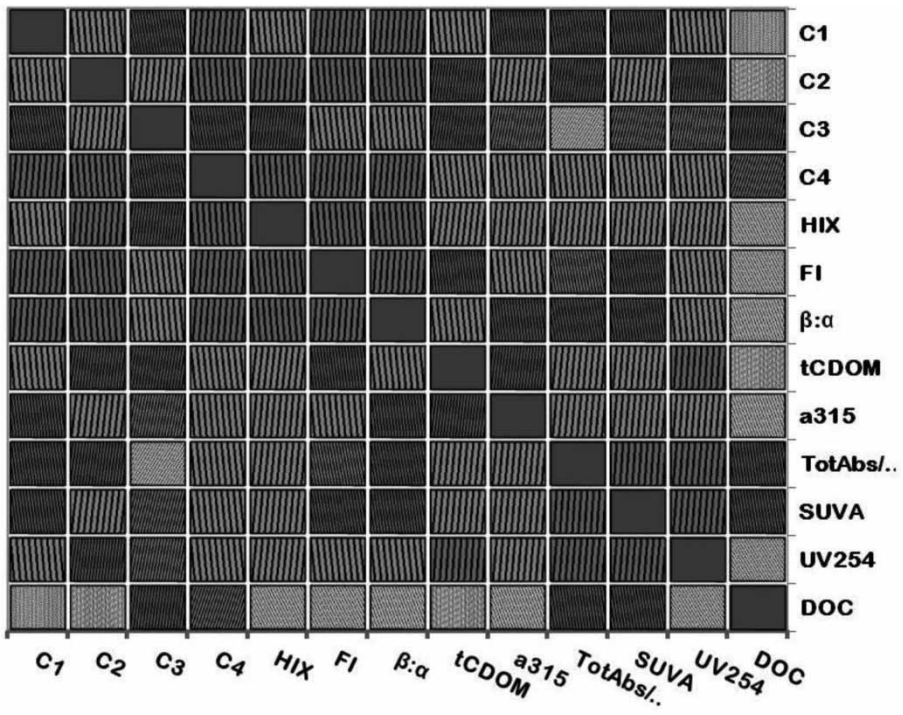

Figure 6 | Correlation map relating NOM removal and spectroscopic parameters.

Water Practice & Technology Vol 15 No 4
doi: 10.2166/wpt.2020.075

(e.g., leachate from algae and bacteria; extracellular release), therefore it is expected that the UV_{254} absorbance coefficient will be relative to the *FI* ratio (Hansen 2014). Previous research reports that terrestrially sourced NOM ($FI > 1.7$) is less likely to be removed by conventional methods than microbially sourced NOM ($FI < 1.3$) (Figure A.2c) (Yu *et al.* 2015). Specific ultraviolet absorbance (SUVA) is calculated as the quotient of UV_{254} absorbance coefficient and the DOC of the sample (Pifer & Fairey 2012). Therefore by definition it is expected that SUVA changes should correlate with UV_{254} absorbance. The UV_{254} reduction and *SUVA* gave a fair relationship ($R = 0.745$). Spectroscopic indices such as *HIX* and *FI* showed strong correlations that exceeded 0.9 with the F_{max} values of C_1 and C_4. This could be because HLM and PLM contains aromatic groups. Aromatic compounds such as humic-like and protein-like NOM fractions tend to be condensed, inferring NOM fractions with a high level of humicity commensurate with *HIX* and *FI* spectroscopic ratios (Kamjunke *et al.* 2016).

Most conventional WTPs regard *DOC* and UV_{254} as the most appropriate surrogate measure of NOM quantity. However, measurement of *DOC* involves the use of expensive instruments and chemicals. There is therefore need for easily measurable parameters that give good correlations with *DOC* so as to act as a surrogate measure for *DOC*. The results indicate spectroscopic indices and *DOC* had a poor correlation. This was because measurement of UV_{254} and spectroscopic ratios rely on NOM moieties that fluoresce or absorb in the *UV-Vis* range, whereas DOC measurement is non-selective of the constituting organic matter (Baghoth Sharma & Amy 2010).

CONCLUSION

The work was motivated by the need to use optical methods to gain insightful understanding of the character of NOM at the three water plants in South Africa with the overarching aim of process optimization. The study revealed that NOM undergoes changes as the water is subjected to different treatment stages. Through *2D-SFS*, it was observed that NOM transformation varied as a consequence of NOM character, the type and dosage of treatment chemicals used, and WTPs' operational parameters.

The key findings were:

1. Humic and fulvic substances dominated coastal plants and were the most amenable for removal by coagulation, as shown by plant H, which had a 42% *DOC* removal at the coagulation stage.
2. The character of NOM at source, coagulation chemicals used, and WTPs' operational parameters play a role in the treatability of NOM, as evidenced by the *2D-SFS* data. Tyrosine-like, tryptophan-like and microbial humic-like substances were degraded or transformed concurrently at plant FB whereas at plant H, fulvic-like matter was transformed first followed by tyrosine-like then humic-like matter.

Because there was a poor correlation between spectroscopic indices and *DOC*, further research needs to focus on determining easily measurable parameters for use as NOM surrogates on a routine monitoring basis such as turbidity, conductivity and pH

DATA AVAILABILITY STATEMENT

All relevant data are included in the paper or its Supplementary Information.

Water Practice & Technology Vol 15 No 4
doi: 10.2166/wpt.2020.075

REFERENCES

Baghoth, S. A., Sharma, S. K. & Amy, G. L. 2010 Tracking natural organic matter (NOM) in a drinking water treatment plant using fluorescence excitation-emission matrices and PARAFAC. *Water Research* **45**(2), 797–809. doi: 10.1016/j.watres.2010.09.005.

Cortina, J. L. & Gonz, S. 2016 Integration of Ultraviolet-Visible spectral and physicochemical data in chemometrics analysis for improved discrimination of water sources and blends for application to the complex drinking water distribution network of Barcelona. *Journal of Cleaner Production* **112**, 4789–4798. doi: 10.1016/j.jclepro.2015.06.074.

Gonçalves-araujo, R., Granskog, M. A., Bracher, A., Azetsu-Scott, K., Dodd, P. A. & Stedmon, C. A. 2016 Using fluorescent dissolved organic matter to trace and distinguish the origin of Arctic surface waters. *Scientific Reports* **6**, 33978. https://doi.org/10.1038/srep33978.

Goslan, E. H. 2003 *Natural Organic Matter Character and Reactivity: Assessing Seasonal Variation in A Moorland Water School of Water Sciences*. PhD Thesis, Cranfield University, Cranfield, UK.

Hansen 2014 *The Effects Of Biodegradation And Photodegradation On Optical Properties Of Dissolved Organic Matter In Aquatic Systems*. *Masters Thesis*, California State University, Sacramento, CA, USA.

Hoffman, L. W., Chilom, G., Venkatesan, S. & Rice, J. A. 2014 Electron and force microscopy characterization of particle size effects and surface phenomena associated with individual natural organic matter fractions. *Microscopy and Microanalysis* **20**(2), 521–530. doi: 10.1017/S1431927614000038.

Hur, J. & Cho, J. 2012 Prediction of BOD, COD, and total nitrogen concentrations in a typical urban river using a fluorescence excitation-emission matrix with PARAFAC and UV absorption indices. *Sensors* **12**(1), 972–986. doi: 10.3390/s120100972.

Hur, J., Jung, K. & Mee, Y. 2011 Characterization of spectral responses of humic substances upon UV irradiation using two-dimensional correlation spectroscopy. *Water Research* **45**(9), 2965–2974. doi: 10.1016/j.watres.2011.03.013.

Jarvis, P. 2004 *The Impact of Natural Organic Matter on Floc Structure*. PhD Thesis, Cranfield University, Cranfield, UK.

Jeong, K., Lee, D.-S., Kim, D.-G. & Ko, S.-O. 2014 Effects of ozonation and coagulation on effluent organic matter characteristics and ultrafiltration membrane fouling. *Journal of Environmental Sciences* **26**(6), 1325–1331. doi: 10.1016/S1001-0742(13)60607-5.

Kamjunke, N., Oosterwoud, M. R., Herzsprung, P. & Tittel, J. 2016 Bacterial production and their role in the removal of dissolved organic matter from tributaries of drinking water reservoirs. *Science of the Total Environment* **548–549**, 51–59. doi: 10.1016/j.scitotenv.2016.01.017.

Kimura, K., Shikato, K., Oki, Y., Kumo, K. & Huber, S. A. 2018 Surface water biopolymer fractionation for fouling mitigation in low-pressure membranes. *Journal of Membrane Science* **554**, 83–89. doi: 10.1016/j.memsci.2018.02.024.

Krasner, S. W., Mitch, W. A., McCurry, D. L., Hanigan, D. & Paul Westerhoff, P. 2013 Formation, precursors, control, and occurrence of nitrosamines in drinking water: a review. *Water Research* **47**(13), 4433–4450. doi: 10.1016/j.watres.2013.04.050.

Krzeminski, P., Vogelsang, C., Meyn, T., Köhler, S. J., Poutanen, H., de Wit, H. A. & Uhl, W. 2019 Natural organic matter fractions and their removal in full-scale drinking water treatment under cold climate conditions in Nordic capitals. *Journal of Environmental Management* **241**, 427–438. doi: 10.1016/j.jenvman.2019.02.024.

Lavonen, E. E., Kothawala, D. N., Tranvik, L. J., Consoir, M., Schmitt-Kopplin, P. & Kohler, S. J. 2015 Tracking changes in the optical properties and molecular composition of dissolved organic matter during drinking water production. *Water Research* **85**, 286–294. doi: 10.1016/j.watres.2015.08.024.

Li, P. & Hur, J. 2017 Utilization of UV-Vis spectroscopy and related data analyses for dissolved organic matter (DOM) studies: a review. *Critical Reviews in Environmental Science and Technology* **47**(3), 131–154. doi: 10.1080/10643389.2017.1309186.

Li, X., Xing, M., Yang, J. & Huang, Z. 2011 Compositional and functional features of humic acid-like fractions from vermicomposting of sewage sludge and cow dung. *Journal of Hazardous Materials* **185**(2–3), 740–748. doi: 10.1016/j.jhazmat.2010.09.081.

Lidén, A., Keucken, A. & Persson, K. M. 2017 Uses of fluorescence excitation-emissions indices in predicting water treatment efficiency. *Journal of Water Process Engineering* **16**, 249–257. doi: 10.1016/j.jwpe.2017.02.003.

Moyo, W., Chaukura, N., Msagati, T. A. M., Mamba, B. B., Heijman, S. G. J. & Nkambule, T. T. I. 2019 The properties and removal efficacies of natural organic matter fractions by South African drinking water treatment plants. *Journal of Environmental Chemical Engineering* **7**(3), 103101. doi: 10.1016/j.jece.2019.103101.

Moyo, W., Chaukura, N., Motsa, M. M., Msagati, T. A. M., Mamba, B. B., Heijman, S. G. J. & Nkambule, T. T. I. 2020 Investigating the fate of natural organic matter at a drinking water treatment plant in South Africa using optical spectroscopy and chemometric analysis. *Water SA* **46**(1), 131–140. 10.17159/wsa/2020.v46.i1.7893.

Murphy, K. R., Hambly, A., Singh, S., Henderson, R. K., Baker, A., Stuetz, R. & Khan, S. J. 2011 Organic matter fluorescence in municipal water recycling schemes: toward a unified PARAFAC model. *Environmental Science and Technology* **45**(7), 2909–2916. doi: 10.1021/es103015e.

Murphy, K. R., Stedmon, C. A., Wenig, P. & Broe, R. 2014 Analytical Methods OpenFluor – an online spectral library of auto-fluorescence by organic compounds in the environment. *Analytical Methods* **3**, 658–661. doi: 10.1039/c3ay41935e.

Najafzadeh, M. & Zeinolabedini, M. 2018 Derivation of optimal equations for prediction of sewage sludge quantity using wavelet conjunction models : an environmental assessment. *Environmental Science and Pollution Research* **25**, 22931–22943. https://doi.org/10.1007/s11356-018-1975-5.

Water Practice & Technology Vol 15 No 4
doi: 10.2166/wpt.2020.075

Najafzadeh, M. & Zeinolabedini, M. 2019 Prognostication of waste water treatment plant performance using efficient soft computing models : an environmental evaluation. *Measurement* **138**, 690–701. doi: 10.1016/j.measurement.2019.02.014.

Ncibi, M. C. & Matilainen, A. 2018 Removal of natural organic matter in drinking water treatment by coagulation : a comprehensive review. *Chemosphere* **190**, 54–71. doi: 10.1016/j.chemosphere.2017.09.113.

Ndiweni, S. N., Chys, M., Chaukura, N., Van Hulle, S. W. H. & Nkambule, T. T. I. 2019 Assessing the impact of environmental activities on natural organic matter in South Africa and Belgium. *Environmental Technology* **40**(13), 3330. doi:10.1080/09593330.2019.1575920.

Nkambule, T. I. 2012 *Natural Organic Matter (Nom) in South African Waters: Characterization of Nom, Treatability and Method Development for Effective Nom Removal From Water*. PhD thesis, University of Johannesburg, Johannesburg, South Africa.

Pifer, A. D. & Fairey, J. L. 2012 Improving on SUVA 254 using fluorescence-PARAFAC analysis and asymmetric flow-field flow fractionation for assessing disinfection byproduct formation and control. *Water Research* **46**(9), 2927–2936. doi: 10.1016/j.watres.2012.03.002.

Pifer, A. D. & Fairey, J. L. 2014 Suitability of organic matter surrogates to predict trihalomethane formation in drinking water sources. *Environmental Engineering Science* **31**(3), 117–126. doi: 10.1089/ees.2013.0247.

Su, B., Qu, Z., He, X. S., Song, Y.-H. & Jia, L.-M. 2016 Characterizing the compositional variation of dissolved organic matter over hydrophobicity and polarity using fluorescence spectra combined with principal component analysis and two-dimensional correlation technique. *Environmental Science and Pollution Research* 9237–9244. doi:10.1007/s11356-016-6173-8.

Vasyukova, E., René Proft, R., Jousten, J., Slavik, I. & Uhl, W. 2013 Removal of natural organic matter and trihalomethane formation potential in a full-scale drinking water treatment plant. *Water Science and Technology: Water Supply* **13**(4), 1099. doi: 10.2166/ws.2013.095.

Wünsch, U. J., Murphy, K. R. & Stedmon, C. A. 2015 Fluorescence quantum yields of natural organic matter and organic compounds: implications for the fluorescence-based interpretation of organic matter composition. *Frontiers in Marine Science* **2**, 1–15. doi: 10.3389/fmars.2015.00098.

Yang, X., Zhou, Z., Raju, N. M., Cai, X. & Meng, F. 2017 Selective elimination of chromophoric and fluorescent dissolved organic matter in a full-scale municipal wastewater treatment plant. *Journal of Environmental Sciences (China)* **57**, 150–161. doi: 10.1016/j.jes.2016.11.003.

Yu, H. 2011 Fluorescence spectroscopic properties of dissolved fulvic acids from salined flavo-aquic soils around Wuliangsuhai in Hetao irrigation district, China. **75**(4), 1385–1393. doi: 10.2136/sssaj2010.0373.

Yu, H., Song, Y., Tu, X., Du, E., Liu, R. & Peng, J. 2013 Assessing removal efficiency of dissolved organic matter in wastewater treatment using fluorescence excitation emission matrices with parallel factor analysis and second derivative synchronous fluorescence. *Bioresource Technology* **144**, 595–601. doi: 10.1016/j.biortech.2013.07.025.

Yu, H., Song, Y., Gao, H., Liu, L., Yao, L. & Peng, J. 2015 Applying fluorescence spectroscopy and multivariable analysis to characterize structural composition of dissolved organic matter and its correlation with water quality in an urban river. *Environmental Earth Sciences* **73**, 5163–5171. doi: 10.1007/s12665-015-4269-y.

Zeinolabedini, M. & Najafzadeh, M. 2019 Comparative study of different wavelet-based neural network models to predict sewage sludge quantity in wastewater treatment plant. *Environmental Monitoring and Assessessment* **191**(163). https://doi.org/10.1007/s10661-019-7196-7.

Zha, X., Liu, Y., Liu, X., Zhang, Q., Dai, R., Ying, L., Wu, J., Wang, J. & Ma, L. 2014 Effects of bromide and iodide ions on the formation of disinfection by-products during ozonation and subsequent chlorination of water containing biological source matters. *Environmental Science and Pollution Research* **21**(4), 2714–2723. doi: 10.1007/s11356-013-2176-x.